Calculation of Infrared Transition Probabilities for the $^1\Sigma^+$ Groundstate of XeH^+

Robert Klein and Pavel Rosmus

Fachbereich Chemie der Universität Frankfurt (Main)

Z. Naturforsch. **39 a**, 349–353 (1984); received January 24, 1984

Near equilibrium potential energy and dipole moment functions have been calculated for the electronic ground state of the XeH^+ ion from highly correlated SCEP/CEPA electronic wavefunctions. The following spectroscopic constants for $^{132}XeH^+$ are obtained:

$R_e = 1.611 \pm 0.005$ Å, $\omega_e = 2313 \pm 50\,cm^{-1}$, $\omega_e x_e = 41 \pm 5\,cm^{-1}$ and $D_0(Xe^+ + H) = 3.90 \pm 0.1$ eV.

Infrared transition dipole matrix elements and probability coefficients for $^{132}XeH^+$ and $^{132}XeD^+$ are given. The electric dipole moment functions of the protonated rare gas atoms HeH^+ to XeH^+ are discussed.

1. Introduction

The object of this paper is to report on the predicted infrared spectrum of XeH^+ and to compare the theoretical electric dipole moment functions of the HeH^+ to XeH^+ ions. For the interpretation of scattering experiments, ion-molecule and charge-exchange reactions, photodissociative processes and astrophysical spectral data the molecular constants of the protonated rare gas atoms are needed, which, however, are not yet reliably established for XeH^+. Recently, vibrational-rotational transitions in the electronic ground states of the ions HeH^+ to KrH^+ have been observed by high resolution spectroscopic techniques. The spectroscopic constants obtained from these experiments are much more accurate than the previous ones from beam scattering [1] or associative ionization [2]. Using fast beam laser spectroscopy and charge-exchange reactions Tolliver et al. [3] measured very accurately the term values of several rotational-vibrational states in HeH^+; their results are in excellent agreement with the accurate adiabatic calculations of Bishop and Cheung [4]. Carrington et al. [5] performed precise measurements of the transitions from bound levels to rotationally quasibound levels of HeH^+. In this experiment the photon transitions were monitored by the detection of the ionic photofragments. Another experimental information on the quasibound levels of the HeH^+ ion comes from the work of Schopman et al. [6], who investigated the momentum distribution of protons produced by rotational predissociation or collisional dissociation. Meanwhile, several direct observations of the infrared radiative transitions have also been reported. Using the difference frequency laser system, Amano et al. [7, 8] observed IR-absorption spectra of HeH^+, NeH^+ and ArH^+. Haese et al. [9] found the IR-absorption band in ArH^+. Brault and Davis [10] detected the IR-emission spectrum of ArH^+ by FT-technique and Johns [11] observed emission in ArH^+ and KrH^+.

So far no experimental values of absolute or relative transition probabilities for these ions are known. For HeH^+ Dobrowski and Herzberg [12] used the near Born-Oppenheimer potential energy function of Kolos [13] and Peak [14] and the Hartree-Fock dipole moment function obtained from the position of the center of negative charges as function of R calculated by Peyerimhoff [15] and Michels [16] and derived theoretical positions, intensities, widths and lifetimes for the bound-bound and bound-quasibound transitions. The positions of the levels below the centrifugal barrier are in excellent agreement with the experimental values of Carrington et al. [5]. For the NeH^+, ArH^+ and KrH^+ ions theoretical potential energy and electric dipole moment functions have been published in our earlier works [17, 18]. The predicted molecular constants for NeH^+, ArH^+ and KrH^+ alleviated the experimental search problem of the infrared transitions in these ions and proved to be good theoretical estimates: for instance, the theoretical $\Delta G_{1/2}$ values

Reprint requests to Doz. Dr. P. Rosmus, Fachbereich Chemie der Universität, Niederurseler Hang, D-6000 Frankfurt (Main).

0340-4811 / 84 / 0400-0349 $ 01.3 0/0. – Please order a reprint rather than making your own copy.

deviate by 7 cm^{-1} for NeH^+, by 24 cm^{-1} for ArH^+ and by 66 cm^{-1} for KrH^+ from the experimental values [8–11]. The calculated intensity data enabled estimates of the average gas phase concentrations from the observed intensities [8]. For the ion XeH^+ only two theoretical calculations [19, 20] have been published which were mainly concerned with the crossing and charge-exchange problem in the electronic ground state but no reliable spectroscopic constants and transition probabilities are so far known.

2. Computational Details

All calculations were carried out with Gaussian-type basis set comprising a total of 112 functions contracted to 94 groups. The exponents and contraction coefficients are listed explicitly in Table 1. The basis set for xenon was roughly optimized in Hartree-Fock calculations so that each core orbital is described by at least two Gaussian functions. Since we were only interested in valence shell properties, the core functions have not been fully optimized with respect to the total energy. The valence shell is described by four s and four p functions with two d and one f polarization functions for xenon and six s with two p and one d polarization function for hydrogen. The correlated electronic wavefunctions were calculated by the SCEP/CEPA method. The SCEP (self-consistent electron pair) [21] approach allows to obtain the solution of Schrödinger equation in the space of all singly and doubly excited configurations with respect to the Hartree-Fock determinant. Higher order substitutions are accounted for by the CEPA (coupled electronpair) [22] approximation. All eight valence electrons have been correlated and we expect that the present calculations cover about 70 per cent of the valence correlation energy. The dipole moments were calculated as expectation values. A basis set of the same size and the SCEP/CEPA method were used for the isoelectronic hydrogen iodide [23]. The latter calculation demonstrates that this theoretical approach is capable to yield spectroscopic constants with an accuracy of about 0.008 Å for R_e, 60 cm^{-1} for ω_e and 0.05 Debye for μ_0. The error bounds of the vibrational dipole matrix elements are expected to be 20 to 30 per cent.

Table 1. Exponents χ_i and contraction coefficients c_i (in parentheses) of the Gaussian type basis set employed:

Xe s:	1086840.5 (0.000304), 162836.5 (0.002354), 37093.27 (0.012206), 10543.936 (0.04849), 3473.113, 1272.956, 519.1500, 228.4260, 88.2555, 32.1873, 16.1975, 7.2681, 2.69958, 1.34979, 0.467235, 0.186894, 0.074758, 0.031149;
Xe p:	8568.05 (0.0022), 2029.88 (0.01763), 648.94 (0.096271), 207.66 (0.401263), 67.489, 20.7660, 7.7873, 3.63405, 1.55745, 0.552376, 0.229464, 0.095524, 0.031149;
Xe d:	186.894 (0.080513), 41.532 (0.502086), 11.837, 3.94554, 1.34979, 0.415320;
Xe f:	0.311490;
H s:	68.16 (0.0255), 10.24 (0.1938), 2.3465, 0.673, 0.2246, 0.082, 0.03;
H p:	0.2, 0.95;
H d:	0.6

3. Results

The protonated rare gas atoms are experimentally generated in a discharge [7–11] or in exothermic reactions [1] in their ground and excited rotational-vibrational states. Thus, both the absorption intensities and the emission rates of these ions are of considerable spectroscopic interest. Moreover, as demonstrated by Dabrowski and Herzberg [12] for HeH^+ the transitions from or to the quasibound levels lying below the centrifugal barriers also give important spectroscopic information. If the protonated rare gas atoms in such a quasibound level are formed in two body collisions, the ions can predissociate again or undergo a radiative transition. In the latter case a new ion is formed and an emission infrared spectrum of the ion results. Such infrared spectra of rare gas atoms are expected in stellar atmospheres or interstellar clouds [12]. For diatomics the transition probabilities, widths and lifetimes can easily be calculated in a good approximation from the potential energy and the electric dipole moment functions.

In Table 2 the calculated SCF and SCEP/CEPA total energies and the dipole moments of the electronic ground state of XeH^+ are listed. The calculated spectroscopic constants are given in Table 3. In this work we restricted our calculations to the near equilibrium region of internuclear distances in which XeH^+ behaves like the other protonated rare gas atoms. At larger internuclear distances another $^1\Sigma^+$ state crosses the ground state potential energy function and the electronic wavefunction changes its character. The XeH^+ ion dissociates into Xe^+ ($^2P_{3/2}$)

and H (^2S). Unlike other protonated rare gas atoms, the dipole moment function of the XeH^+ ion will have a maximum at large internuclear distances accompanied by a change of the positive charge transfer back to xenon. Similarly the dipole moment function of the isoelectronic hydrogen iodide is qualitatively different from those of other hydrogen halides [23]. It has a very small negative first derivative at R_e and exhibits no maximum at longer distances.

To our knowledge the only empirical data concerning the potential energy function of the XeH^+ ground state have so far been published by Mittmann et al. [24] who investigated the proton scattering on xenon. These authors derived an equilibrium distance of 1.74 Å for XeH^+ and a dissociation energy of 6.75 eV. Since the proton scattering results turned out to be energy dependent – probably because of charge-exchange in the curve crossing region – these constants are very uncertain. From Hartree-Fock calculations Kubach and Sidis [19] obtained a dissociation energy (D_e) of 4.33 eV ($Xe^+ + H$). Valence bond calculations performed by Gallup and Macek [20] led to a value of 2.2 eV. According to other calculations of proton affinities by means of the CEPA method [25] our D_e value of 4.05 eV ($Xe^+(^2P_{3/2}) + H(^2S)$) should exhibit error bounds of about ± 0.1 eV. The Tables 4 and 5 some vibrational dipole matrix elements and Einstein coefficients of spontaneous emission for $^{132}XeH^+$ and $^{132}XeD^+$ are listed. We have also calculated the transition probabilities for all other xenon isotopes since the natural abundance of these isotopes will complicate the fine structure and assignments of XeH^+ rotation-vibration spectra. It should be noted that each isotope combination has a different dipole moment function in molecular ions. The calculations show that the mass difference between the isotopes from ^{129}Xe to ^{136}Xe cause a change of the intensities of less than 1%, i.e. all intensities will parallel the natural abundances of xenon isotopes. Similar behavior has been found for KrH^+.

In Fig. 1 the electric dipole moment function referred to the center of mass of the most abundant

Table 2. Calculated potential energy and dipole moment functions for ground state of XeH^+.

R (a. u.)	Potential energy (a. u.)		Dip. mom. (a. u.)	
	HF	SCEP/CEPA	HF	SCEP/CEPA
2.5	−7227.161006	−7227.319565	0.46663	0.42826
2.7	−7227.193904	−7227.352913	0.53730	0.49261
2.8	−7227.202510	−7227.361811	0.57912	0.52977
3.0	−7227.209136	−7227.369161	0.67596	0.61320
3.2	−7227.206295	−7227.367231	0.79053	0.70719
3.4	−7227.197836	−7227.359860	0.92284	0.80912
3.8	−7227.173120	−7227.337741	1.23940	1.02356
4.2	−7227.146022	−7227.313470	1.62047	1.22782

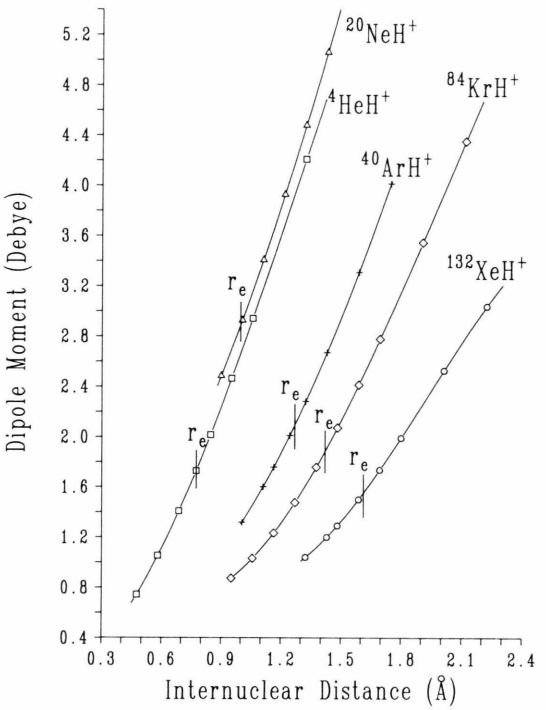

Fig. 1. Electric dipole moment functions calculated from CEPA electronic wavefunctions of the protonated rare gas atoms (with respect to the center of mass as origin of the coordinate system).

Table 3. Calculated spectroscopic constants, dissociation energies, dipole moments and dipole moment derivatives of the ground state of XeH^+.

Method	R_e (Å)	B_e (cm^{-1})	α_e (cm^{-1})	ω_e (cm^{-1})	$\omega_e x_e$ (cm^{-1})	D_0 (eV)	μ_e (D)	μ'_e (D/Å)
HF	1.601	6.58	0.168	2401.1	38.22	3.41	1.693	2.554
SCEP/CEPA	1.611	6.49	0.180	2313.6	41.2	3.90	1.551	2.159

Table 4. Vibrational[a] dipole matrix elements (lower triangle and diagonal elements; in Debye) and Einstein coefficients of spontaneous emission (upper triangle; in sec^{-1}) of $Xe^{132}H^+$ ($X^2\Sigma^+$).

v'' \ v'	0	1	2	3	4	5
0	1.597	125	1.96	0.05		
1	0.189	1.695	235	7.2	0.08	
2	-0.863×10^{-2}	0.275	1.796	331	17.2	0.08
3	-0.773×10^{-3}	−0.0174	0.344	1.899	408	33.4
4		-0.106×10^{-2}	−0.0285	0.405	2.004	466
5			-0.109×10^{-2}	−0.0421	0.458	2.107

[a] The vibrational spacings and eigenfunctions have been obtained from the solution of the radial Schrödinger equation with the fitted SCEP/CEPA potential energy function as input. The dipole moment function has been referred to the center of mass.

Table 5. Vibrational dipole matrix elements (lower triangle and diagonal elements; in Debye) and Einstein coefficients of spontaneous emission (upper triangle; in sec^{-1}) of $Xe^{132}D^+$ ($X^2\Sigma^+$).

v'' \ v'	0	1	2	3	4	5
0	1.522	31	0.29	0.01		
1	0.156	1.529	60	1.05	0.02	
2	-0.543×10^{-2}	0.225	1.662	86	2.4	0.03
3	-0.602×10^{-3}	0.0107	0.280	1.732	110	4.7
4		-0.889×10^{-3}	−0.0170	0.329	1.804	130
5			-0.111×10^{-2}	−0.0244	0.373	1.876

Table 6. Theoretical electrical dipole moment function He^4H^+ (all values in a.u.)[a].

R	HF-SCF	SCEP
0.9	0.4794	0.4736
1.1	0.6462	0.6356
1.3	0.8328	0.8157
1.4632	0.9978	0.9747
1.6	1.1435	1.1154
1.8	1.3664	1.3320
2.0	1.5980	1.5595
2.5	2.1947	2.1587

[a] Calculated with a basis set of the size 7 s, 3 p, 2 d for He and 7 s, 2 p, 1 d for H. The dipole moments refer to He in the origin. The SCEP total energy at the calculated R_e amounts to −2.97517 hartrees. The near Born-Oppenheimer total energy at R_e of Kolos and Peek [14] was calculated to be −2.97869 hartrees.

isotopes of the protonated rare gas atoms are drawn. Since Dobrowski and Herzberg [12] evaluated the dipole moment functions for HeH^+ only from Hartree-Fock results of Peyerimhoff [15] and Michels [16], we have recalculated this function using a correlated SCEP wave function. These results are presented in Table 6. In HeH^+ the correlation contributions to the dipole moment are small. Hence our μ_e value deviates by only 0.15 Debye from that obtained by Dobrowski and Herzberg (cf. also Table 7). However, the intention of these calculations was to make sure that the dipole moment function of HeH^+ lies below that of NeH^+. It turned out that NeH^+ has the largest dipole moment of all protonated rare gas atoms. Figure 1 shows that the R-dependent charge transfer increases in the sequence Xe, Kr, Ar, Ne, whereas HeH^+ represents an exception in this systematic behavior. All rare gas hydride cations have larger dipole moments in their vibrational ground states than their isoelectronic neutral counterparts (HF: 1.827 D; HCl: 1.109 D; HBr: 0.828 D; HI: 0.447 D), i.e. they will have intense rotational transitions in the microwave spectra. Also the first derivatives at equilibrium distance which determine the magnitude of the transition dipole matrix elements in the fundamental sequence $\Delta v = 1$ are larger in these ions than in the isoelectronic neutrals.

The slope of the dipole moment functions referring to the rare gas atoms in the origin of the coordinate system approaches the limiting value one with increasing internuclear distance if both μ and R are given in atomic units. Transforming the function so that it refers to the center of mass in the

Table 7. Comparison of experimental and theoretical spectroscopic data of the protonated rare gas atoms in their electronic ground states.

Species	Method	Ref.	r_e (Å)	ω_e (cm^{-1})	D_0 (eV)	μ_e (D)	μ'_e (D/Å)	A_0^1 (sec^{-1})[a]	lim μ' (D/Å)
He^4H^+	theory	4, 12	0.7743	3228.4	1.845	1.729[b]	3.86[b]	837[b]	3.59[b]
$Ne^{20}H^+$	exp.	7, 2	0.9913	2900	2.101 ± 0.03				
	theory	18	0.996	2896	2.104	2.885	4.34	756	3.901[b]
$Ar^{40}H^+$	exp.	10, 2	1.2804	2711.0	3.856 ± 0.03				
	theory	17	1.286	2723	3.89	2.093	3.369	438	4.685[b]
$Kr^{84}H^+$	exp.	11, 1	1.4212	2494.65	4.29				
	theory	18	1.419	2561	4.65	1.883	2.94	285	4.774[b]
$Xe^{132}H^+$	theory[b]		1.611	2313	3.90	1.551	2.16	125	(4.767)[c]

[a] Einstein coefficients of spontaneous emission for $(v = 1) \rightarrow (v = 0)$ transitions.
[b] This work. [c] Assuming dissociation into Xe and H^+.

origin, this value becomes

$$\lim \mu' = 1 - m_H/(m_A + m_H) .$$

For the most abundant isotopes these lim μ's are also listed in Table 7. Since both the ΔG values and the first derivatives of $\mu(R)$ at equilibrium distance increase with decreasing atomic mass of the rare gas atoms (cf. Table 7), the HeH^+ ion is calculated to be the best absorber and emitter among the protonated rare gas atoms. The infrared intensities are much larger and the radiative lifetimes smaller than those of the isoelectronic neutrals. For instance, the vibrational emission rates [23, 26] for $v = 1$ amount to 189 sec^{-1} in HF, 34 sec^{-1} in HCl, 5 sec^{-1} in HBr and 0.1 sec^{-1} in HI, the corresponding values of the ions are an order of magnitude larger (cf. Table 7). Due to the rather linear shape of these functions near the equilibrium distances the emission intensities of all protonated rare gas atoms will be dominated by the fundamental sequence $\Delta v = 1$, whereas the first overtone $\Delta v = 2$ and higher overtones will be much less intense. Because of their large transition energies and steep electric dipole moment functions, the protonating modes will belong to the most intense rotational-vibrational transitions within the electronic states in the infrared spectral region.

Acknowledgements

The support of the Deutsche Forschungsgemeinschaft and the Fonds der chemischen Industrie is gratefully acknowledged. Thanks are due to the Hochschulrechenzentrum der Universität Frankfurt for providing their computer facilities and to Prof. Dr. E. A. Reinsch and Doz. Dr. H.-J. Werner for their SCEP/CEPA program.

[1] A. Henglein, J. Phys. Chem. **76,** 3883 (1972) and references therein.
[2] J. Lorenzen, H. Hotop, M. W. Ruf, and M. Morgner, Z. Phys. A **297,** 19 (1980).
[3] D. E. Tolliver, G. A. Kyrala, and W. H. Wing, Phys. Rev. Lett. **43,** 1719 (1979).
[4] D. M. Bishop and L. M. Cheung, J. Mol. Spec. **75,** 462 (1972).
[5] A. Carrington, J. Buttenshaw, R. A. Kennedy, and T. P. Softley, Mol. Physics **44,** 1233 (1981), cf. also A. Carrington, R. A. Kennedy, T. P. Softley, P. G. Fournier, and E. G. Richard, Chem. Phys. **81,** 251 (1983).
[6] J. P. Schopman, P. G. Fournier, and J. Los, Physica **63,** 518 (1973).
[7] P. Bernath and T. Amano, Phys. Rev. Lett. **48,** 20 (1982).
[8] M. Wong, P. Bernath, and T. Amano, J. Chem. Phys. **77,** 693 (1982).
[9] N. H. Haese, F. S. Pan, and T. Oka, Phys. Rev. Lett. **50,** 1575 (1983).
[10] J. W. Brault and S. P. Davis, Phys. Scr. **25,** 26 (1982).
[11] J. W. C. Johns, private communication.
[12] I. Dobrowski and G. Herzberg, Transactions of the New York Academy of Sciences **38,** 14 (1977).
[13] W. Kolos, Int. J. Quantum Chem. **10,** 217 (1976).
[14] J. M. Peek and W. Kolos, Chem. Phys. **12,** 381 (1976).
[15] S. Peyerimhoff, J. Chem. Phys. **43,** 998 (1965).
[16] H. H. Michels, J. Chem. Phys. **44,** 3834 (1966).
[17] P. Rosmus, Theor. Chem. Acta **51,** 359 (1979).
[18] P. Rosmus and E.-A. Reinsch, Z. Naturforsch. **35 a,** 1066 (1980).
[19] C. Kubach and V. Sidis, J. Phys. B **6,** L 289 (1973).
[20] G. A. Gallup and J. Macek, J. Phys. B **10,** 1601 (1977).
[21] W. Meyer, J. Chem. Phys. **64,** 2901 (1976).
[22] W. Meyer, J. Chem. Phys. **58,** 1017 (1973).
[23] H.-J. Werner, E.-A. Reinsch, and P. Rosmus, Chem. Phys. Lett. **78,** 311 (1981).
[24] H. U. Mittmann, H. P. Weise, A. Ding, and A. Henglein, Z. Naturforsch. **26 a,** 1112 (1971).
[25] P. Rosmus and W. Meyer, J. Chem. Phys. **66,** 13 (1977).
[26] H.-J. Werner and P. Rosmus, J. Chem. Phys. **73,** 2319 (1980).